Iranian Polymer Journal (2020) 29:841–851
https://doi.org/10.1007/s13726-020-00844-2

ORIGINAL RESEARCH

Improvement of physical and mechanical properties of electrospun poly(lactic acid) nanofibrous structures

Homa Maleki[1] · Rouhollah Semnani Rahbar[2] · Ahsan Nazir[3]

Received: 4 March 2020 / Accepted: 7 July 2020 / Published online: 13 July 2020

Abstract

The electrospinning of stereocomplexed poly(lactic acid) (Sc-PLA) twisted yarns was our approach to produce PLA-based nanofibrous structures with improved physical and mechanical characteristics for the applications as medical devices. An electrospinning apparatus consisted of two nozzles, and a take-up/twister unit was employed to fabricate twisted yarns through a continuous procedure. The yarn samples were produced via electrospinning of the solutions of high molecular weights poly(D-lactide) (PDLA) and poly(L-lactide) (PLLA) and also their blend solution at 1:1 ratio, and their physical and mechanical properties were compared. The morphological studies indicated that uniform yarns composed of bead-free and smooth fibers were formed. Electrospinning of the blend solution of PLLA/PDLA resulted in developing fibers and yarns with smaller diameters. The DSC analysis showed that the Sc-PLA yarn had a higher melting peak (at 230 °C) compared to PLLA and PDLA samples (184 °C), indicating the formation of stereocomplex crystallites in this sample. After isothermal heat treatment, the formation of the stereocomplex crystals in the electrospun Sc-PLA yarn was also confirmed by FTIR and WAXD analyses. Furthermore, because of the formation of stereocomplex crystallites during the electrospinning process, the stress-at-break and Young's modulus of the yarns were enhanced, while the strain-at-break (%) was reduced. The current approach of stereocomplexation during the electrospinning procedure, and simultaneously, collecting the stereocomplexed nanofibers in the form of twisted yarn, can improve the inherent lack of physical and mechanical features of PLA nanofibrous structures for advanced applications as medical textiles.

✉ Homa Maleki
hmaleki@birjand.ac.ir

[1] Faculty of Arts, University of Birjand, University Blvd., Birjand 9717434765, Iran

[2] Department of Textile and Leather, Chemistry and Petrochemistry Research Center, Standard Research Institute (SRI), P. O. Box 31745-139, Karaj, Iran

[3] Faculty of Engineering and Technology, National Textile University, Faisalabad, Pakistan

Graphic abstract

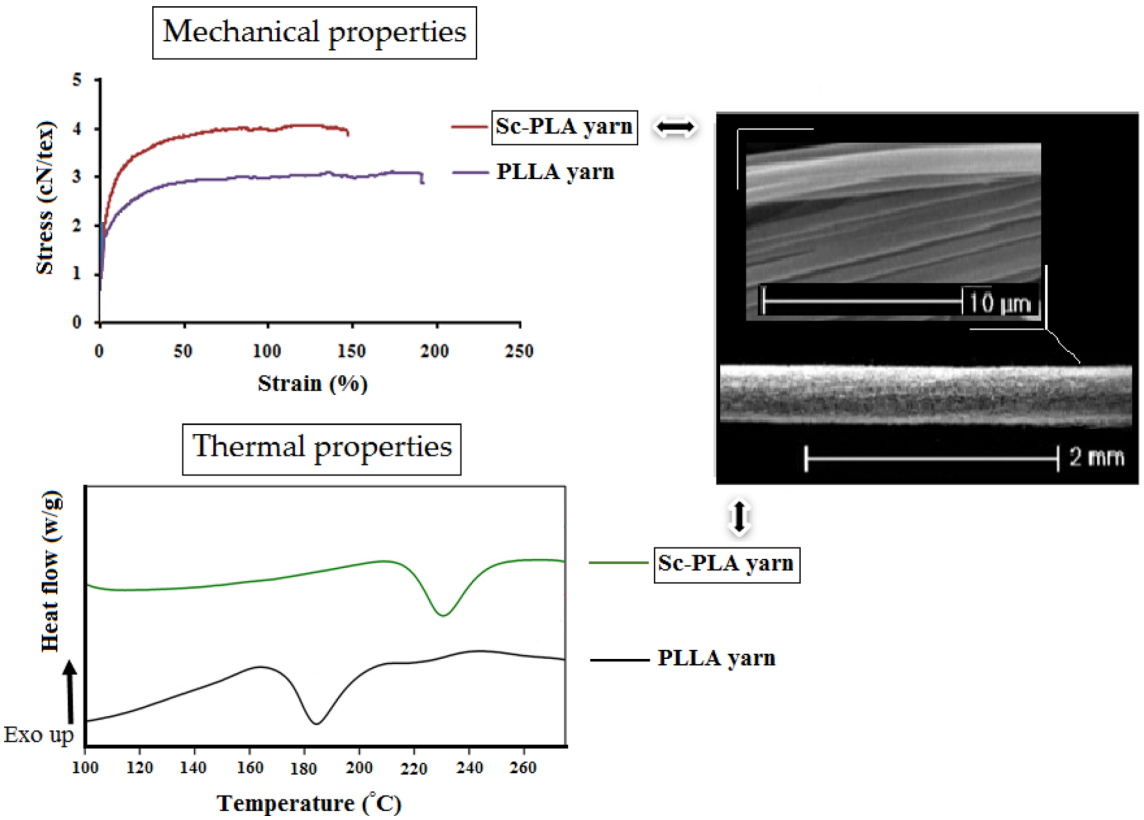

Keywords PLA stereocomplex · Electrospinning · Yarn · Mechanical property · Heat resistance

Introduction

Electrospinning is recently proposed as an efficient technique to produce polymeric nanofibrous structures for biomedical applications. Electrospun fibrous materials generally exhibit several excellent features, such as high porosity with tiny pore size, and high surface area to volume ratio. Further, the electrospinning method by applying different materials and tuning the process variables enables diverse options by regulating the fiber characteristics such as morphology, diameter, and network porosity. These characteristics have developed their potential application as novel biomaterials in regenerative medicine [1, 2].

To this point, different natural and synthetic polymers have been employed for electrospinning of the nanofibers. Poly(lactic acid) (PLA) is a biocompatible, biodegradable, and non-toxic hydrophobic aliphatic polyester with desired thermomechanical properties, which make it a suitable candidate to produce various medical devices [1, 3].

However, PLA-based nanofibrous structures have several limitations that significantly restrict their applications. Firstly, PLA polymer has a low thermal resistance that can be a serious problem when used as a medical textile material. Moreover, it is very brittle with a low impact toughness, which is a drawback in mechanically intensive applications, such as medical implants. PLA is hydrolytically sensitive that may hinder its efficiency on prolonged procedures under physiological conditions [4–6]. Hence, from this point of view, the improvement of the physical and mechanical properties of PLA nanofibers is a vital issue for their applications as biomedical textiles.

Different research works have been proposed to control the PLA's physical constraints. Stereocomplexation, which was reported by Ikada et al. for the first time in 1987 [7], has emerged as an appropriate strategy to overcome these limitations. This phenomenon has attracted growing attention and presented a novel approach to design and develop the PLA-based functional biomaterials with specified and tunable properties such as degradation behavior, thermal stability, and mechanical performance [8, 9].

PLA stereocomplex (Sc) can be obtained by crystallization of the blend of enantiomers of poly(L-lactide) (PLLA) and poly(D-lactide) (PDLA) in solution or under melting state, at a specific polymer concentration. Apart from the

more compact structure and higher melting temperature of the stereocomplex crystals than PLA homopolymers, formation of Sc also endows PLA-based materials with improved mechanical function, thermal stability, and hydrolysis resistance [10–12].

The stereocomplexation process dramatically depends on the molecular weight of the homopolymers. It is not easy to gain stereocomplex crystals from high molecular weight polymers via conventional procedures, whereas the high molecular weight is required for improving mechanical function [13–15]. Several efforts have been performed to produce PLA stereocomplexed fibers via the solution or melt spinning. However, in the fibers produced by these methods, the homocrystallites had also been formed beside the stereocomplex crystallites [16]. Tsuji et al. [17] conceived that the electrical field during the electrospinning process might boost the molecular chain orientation in the polymer and thus increase the probability of stereocomplex crystallites growth and suppress the homocrystallites formation, even using high molecular weight PLA homopolymers. For the first time, they applied the electrospinning technique to produce PLA stereocomplex crystallites in the nanofibers. The fibers were electrospun from the PLLA/PDLA mixed solution prepared by dissolving their cast film in chloroform. Using this strategy, various research works have been performed to overcome the PLA limitations by forming stereocomplex crystallites in the PLA electrospun fibers [18–20].

Nevertheless, there are some problems that limit the further development of Sc-PLA nanofibrous materials. In all of these research works, due to the helix nature of the jet in the typical electrospinning, Sc-PLA nanofibers are collected in the form of web with a random fiber orientation useful as tissue engineering scaffolds, wound dressing materials, membranes and drug carriers [15, 21–23]. The low mechanical strength and the trouble in the tailoring of such random fibrous webs have confined their efficiency in many biomedical applications. Thus, it is however, a serious challenge to produce PLA nanofibrous structures with enhanced mechanical strength beside optimal structural integrity and uniformity.

Aiming to provide the requirements for specific load-bearing applications in biomedical engineering, the mechanical properties of the nanofibrous structures have to be tuned, which is the main goal of the presented work. Different from the other research works, in the present work, our approach is to electrospun stereocomplexed PLA aligned structures in the form of twisted yarns. Due to the state of alignment of the nanofibers in yarn, and also increased cohesion and inter-fiber interaction forces, the mechanical performance of these structures will be significantly improved [24–26].

In the current study, aiming to modify the physical and mechanical performance of PLA nanofibrous structures as implantable medical devices, the fabrication and properties of stereocomplexed PLA nanofibrous yarns by a continuous process is presented. An electrospinning apparatus consisting of two nozzles used to produce stereocomplexed PLA (Sc-PLA) twisted yarns from a blend solution of high molecular weight enantiomers of PLLA and PDLA (1:1 ratio). It was reported that the stereocomplex with a minimum amount of homocrystals was obtained at a blending ratio of 1:1 [17, 18]. These 3-dimensional nanofibrous structures with enhanced physical and mechanical properties will develop advanced medical applications in the form of high performance and functional textiles, weaved and knitted structures, tissue engineering scaffolds, drug carriers, artificial blood vessels, and sutures or other implants. The art of altering the process parameters (twisting rate, take-up speed, etc.), solution properties (solvent type, concentration, etc.), and the blend ratio of PLLA/PDLA, enabled us to innovate and control the degradation rate, and physical–mechanical behavior of Sc-PLA nanofibrous biomaterials. The physical and mechanical characteristics of Sc-PLA electrospun yarns were described and compared with those of PLLA, PDLA, or hybrid PLLA/PDLA yarns. The morphology of electrospun fibers and yarns was considered using scanning electron microscopy (SEM) and atomic force microscopy (AFM) techniques. Differential scanning calorimetry (DSC) was used to investigate the thermal characteristics of the samples. The crystalline structure of the samples was investigated by Fourier transform infrared spectroscopy (FTIR) and wide-angle X-ray diffraction (WAXD) analyses. The mechanical performance of the electrospun yarns was studied by tensile testing.

Experimental

Materials

Poly(l-lactide) (intrinsic viscosity of 2.51 dL/g and $M_w \sim 3 \times 10^5$ g/mol) and Poly(d-lactide) (inherent viscosity of 2.40 dL g^{-1} and $M_w \sim 2.9 \times 10^5$ g mol^{-1}) were supplied from Purac Biomaterials, Netherlands. Specific optical rotation values of PLLA and PDLA were − 158.3 dm^{-1} g^{-1} cm^3 and 158.7 dm^{-1} g^{-1} cm^3 (chloroform, 20 °C), respectively. By considering specific optical rotation values of PLLA and PDLA and their reference values, the content of d-isomer or l-isomer could be calculated according to the proposed equation by Mei et al. [19]. The d-isomer content of the PLLA was approximately 0.7%. The l-isomer content of the PDLA was approximately 0.9%. The polydispersity indices (M_w/M_n) of PLLA and PDLA were 2.0 and 1.8, respectively. 2,2,2-Trifluoroethanol (TFE) (Merck, Germany) selected as a solvent for the preparation of polymer solutions.

Polymer solutions

To fabricate the stereocomplexed PLA (Sc-PLA) nanofibrous yarns, PLLA and PDLA were first individually dissolved in 2,2,2-trifluoroethanol (TFE) to reach 7 wt% concentration. After vigorous stirring at 40 °C for at least 3 h, the same volumes of PLLA and PDLA solutions were mixed to obtain the PLLA/PDLA blend ratio of 1:1. To obtain homogeneity, the blend solution was stirred at 40 °C for at least 3 h and used as the spinning dope for the preparation of the PLA stereocomplex nanofibers.

Electrospinning

To produce PLA yarns, a previously described electrospinning device equipped with two nozzles and a take-up/twister unit was employed [26–28]. The nozzles were placed at a distance of 30 cm from the take-up unit. The polymer solutions were delivered to needles (22-gauge, ID = 0.4 mm, OD = 0.7 mm) by digitally controlled syringe pumps at a flow rate of 0.3 mL h^{-1}. The distance between two needles set at 30 cm. The needles were oppositely charged with a voltage of 13 kV. The twister rotation speed was set at 240 rpm to twist the fibers around the yarn axis. Simultaneously, the fabricated yarn was collected by the take-up roller installed on the twister plate. The linear take-up rate set to 2.4 m/h. To produce hybrid PLLA/PDLA yarn samples, the PDLA solution was fed to the positively charged needle, and the PLLA fibers were spun from the negatively charged needle.

Characterization

The morphology of the electrospun yarns was studied by a scanning electron microscope (SEM; XL 30, Philips, Netherlands) at an accelerating voltage of 25 kV. Before the analysis, samples were coated with a thin layer of gold. From the SEM micrographs, the diameter of the fibers and yarns were measured using Digimizer 4.1.1.0 software, and the reported results of 100 measurements were recorded. A bioscope catalyst atomic force microscopy (AFM) (Bruker AXS, USA) was used to observe the surface morphology of individual electrospun fibers at a scan rate of 1 Hz. Differential scanning calorimetry (DSC) (Mettler SW 9.01, Switzerland) was used to confirm the formation of stereocomplex between PDLA and PLLA. The thermal behaviors of the PLLA, PDLA, and Sc-PLA electrospun yarns were measured by heating at a rate of 10 °C/min from 25 to 250 °C under nitrogen protection. Fourier transform infrared spectroscopy (FTIR) spectra of samples were recorded on a Shimadzu FTIR spectrometer (Japan) in the range of 400–4000 cm^{-1}, and at the resolution of 4 cm^{-1}. The crystalline reflections were characterized with a Bruker D8 ADVANCE- X-ray diffractometer (XRD) (USA) in the scanning range of $2\theta = 5–80^{\circ}$. The wavelength of the X-ray was 0.154 nm. Mechanical function of the electrospun yarns was investigated using a tensile tester (Instron Elima EMT-3050, Iran) at an applied gauge length of 20 mm and 10 mm min^{-1} crosshead speed. The stress-at-break and Young's modulus data were reported in cN per tex (cN/tex). The results of 20 measurements were averaged.

Results and discussion

In this study, a double-nozzle electrospinning set-up was employed to produce twisted yarns. The serious challenge of this mechanism was to produce a uniform yarn, in a continuous process without yarn breakage. Previous studies showed that type of solvent is the most critical factor influencing the spinnability, morphology, mechanical, and physical properties of the electrospun PLA yarns [29]. The electrospinning of PLLA with solvents such as dichloromethane (CH_2Cl_2) or chloroform ($CHCl_3$) resulted in a non-uniform yarn composed of fibers with porous surfaces.

During the electrospinning of PLA/2,2,2-trifluoroethanol (TFE), a stable jet was formed, and uniform yarns and fibers with smooth morphology and narrow diameter distribution were produced. The electrospun PLLA yarns made from TFE showed enhanced mechanical properties compared to those spun with the other solvents. Moreover, when using TFE as a solvent, due to higher conductivity of PLLA/TFE solution (0.4 μS cm^{-1}) than dichloromethane (0.2 m^{-1}) or chloroform (0.1 μS cm^{-1}), a lower voltage was required [29, 30].

Afterward, a series of preliminary experiments were performed to determine the optimum conditions for electrospinning of PLA/TFE yarns. The effective values of 7 wt% concentration, linear take-up speed of 2.4 m/h, and the twisting rate of 240 rpm, allowed uniform yarn formation with a continuous process.

Morphology

The morphology of the PLA-based electrospun fibers and yarns can be deduced from SEM micrographs in Fig. 1. The uniform twisted yarns composed of defect-free, beadles, and uniform nanofibers with a narrow diameter distribution were collected though the electrospinning process (Fig. 1a–d). Higher magnification images show the state of alignment of the nanofibers in the yarn structure, where fibers were arranged with an angle to the yarn axis.

The average diameter of the yarns and corresponding fibers measured from SEM micrographs are reported in Table 1. The results indicate that the formation of Sc was resulted in a smaller diameter of fibers and yarns. As can be

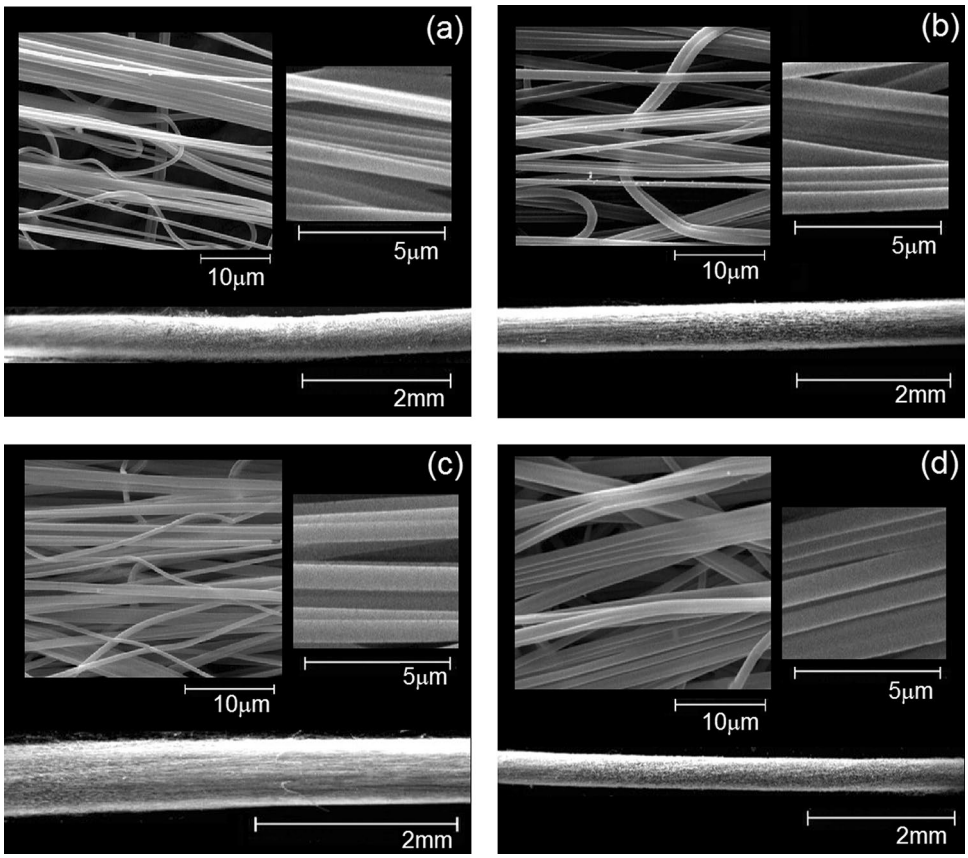

Fig. 1 SEM micrographs of electrospun yarns: **a** PLLA, **b** PDLA, **c** hybrid PLLA/PDLA, and **d** Sc-PLA

Table 1 Mean diameter of electrospun fibers and corresponding yarns

Yarn sample	Fiber diameter (nm) ± SD	Yarn diameter (μm) ± SD
PLLA	754 ± 121	586 ± 26
PDLA	740 ± 107	573 ± 27
Hybrid PLLA/PDLA	772 ± 120	768 ± 145
Sc-PLA	606 ± 106	445 ± 16

seen, Sc-PLA yarns had a smaller diameter (445 ± 16 μm) than those produced from PLLA or PDLA. In the case of solutions electrospun from PLLA or PDLA, yarns with diameters of 586 ± 26 and 573 ± 27 μm were produced, respectively. The hybrid PLLA/PDLA yarns showed the highest average diameter of 768 ± 145 μm. The statistical analysis also confirmed this trend ($p \leq 0.05$). Electrospinning of PLLA and PDLA solutions formed nanofibers with mean diameters of 754 ± 121 nm and 740 ± 107 nm, respectively (Table 1), while the fibers produced from Sc-PLA solutions showed a smaller diameter of 606 ± 106 nm.

Considering the detailed surface morphology, the AFM analysis of the single fibers was performed for PLLA, PDLA, and Sc-PLA electrospun fibers. The AFM images in Fig. 2 clearly show that the electrospun fibers have a cylindrical shape with a surface that was not entirely smooth but consisting of few small grooves with nanometer-sized pores.

Thermal properties

The formation of stereocomplex crystallites through electrospinning of the PLLA/PDLA blend solution was considered by differential scanning calorimetry and the corresponding DSC curves of the yarn samples for the first heating scans are presented in Fig. 3. Thermal characteristics of the electrospun PLA yarns extracted from DSC thermograms, consisting of melting temperature (T_m), onset of melting, and melting enthalpy (ΔH_m) have been reported in Table 2.

As can be observed from Fig. 3, the DSC curves of the electrospun PLLA and PDLA yarns exhibited an endothermic peak at around 184 °C, related to the melting of the homocrystallites (Fig. 3a, b). Similar behavior was also found for the hybrid PDLA/PLLA yarn (Fig. 3c), while, Sc-PLA sample showed a melting peak at 230 °C (Fig. 3d). This confirmed that stereocomplex was formed and strong interaction between PLLA and PDLA chains increased the melting temperature of the Sc-PLA yarns by about 56 °C compared to PLLA and PDLA samples.

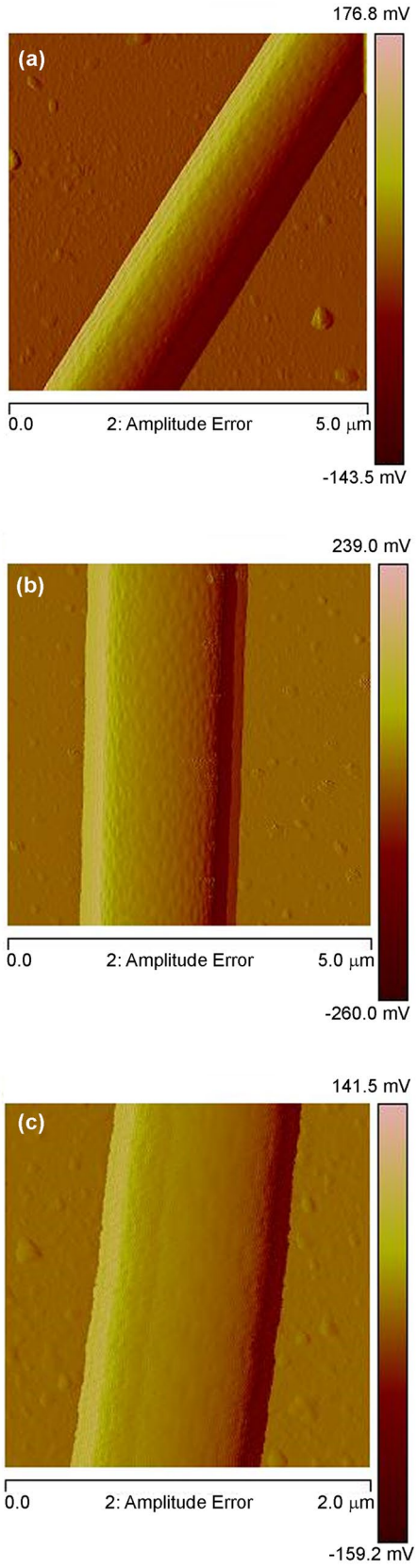

Fig. 2 AFM images of electrospun fibers: **a** PLLA, **b** PDLA, and **c** Sc-PLA

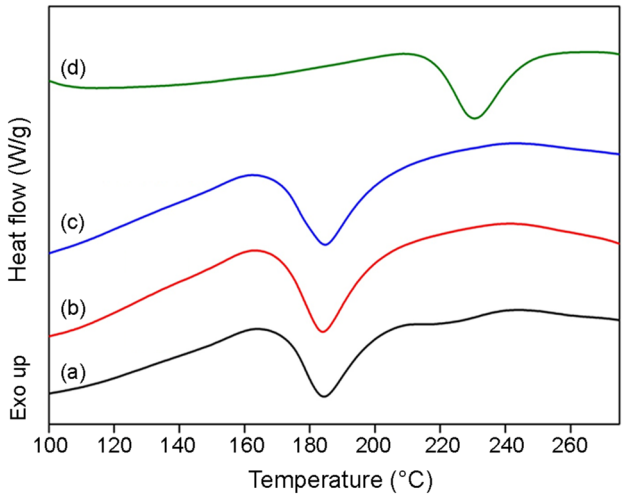

Fig. 3 DSC curves of electrospun yarns: **a** PLLA, **b** PDLA, **c** hybrid PLLA/PDLA, and **d** Sc-PLA

Table 2 Thermal properties of electrospun yarns

Yarn sample	Onset of melting (°C)	Melting temperature (T_m) (°C)	Melting enthalpy (ΔH_m) (J/g)
PLLA	173.0	184.4	23.29
PDLA	171.2	184.1	34.34
Hybrid PLLA/PDLA	170.8	184.9	26.57
Sc-PLA	218.2	230.7	23.23

DSC thermograms of the Sc-PLA electrospun yarns did not show any characteristic of homopolymers, and also no melting transition at around 184 °C, which confirmed that the stereocomplex crystals of the polylactides were successfully formed in the Sc-PLA samples (Fig. 3d). During the electrospinning process, the feasibility of the stereocomplex crystallites formation was increased. The higher alignment and orientation of the molecular chains due to the high applied voltage suppressed the homocrystallites formation. Moreover, the electrical field enforces an additional stretching, which increases the surface area of molecular chains and thus the interaction between PLLA and PDLA chains [17, 31].

FTIR

FTIR spectroscopy was found as a useful method for investigating the PLA stereocomplex crystals. Figure 4a shows stretching in the $-CH_3$ rocking vibrations in the 960−880 cm^{-1} for the as-spun samples. As can be seen, there is no crystalline peak for nascent electrospun PLA yarns, indicating they are almost amorphous. This suggests

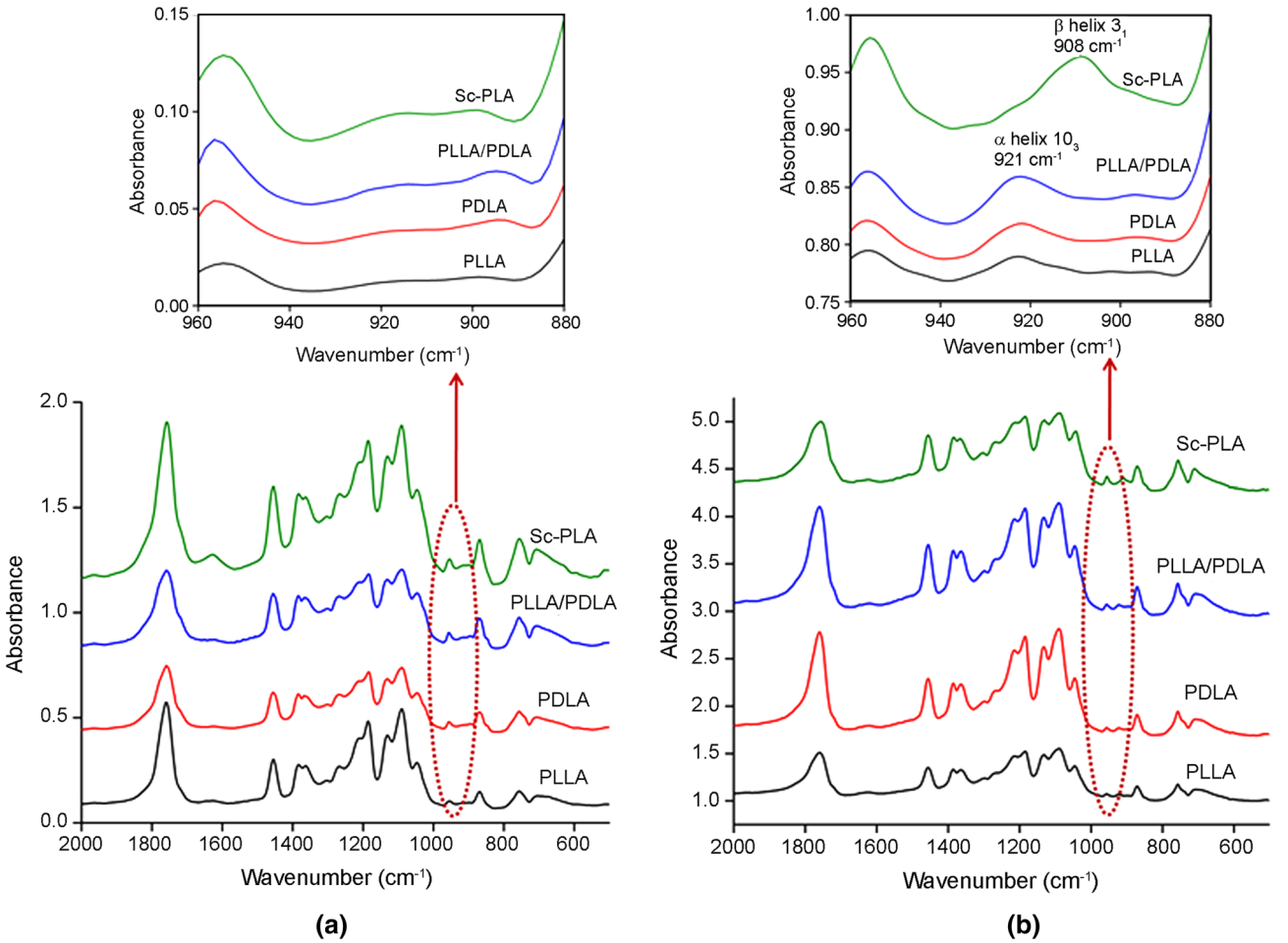

Fig. 4 FTIR spectra of the electrospun yarns before (**a**) and after (**b**) heat treatment at 80 °C for 2 h obtained from PLLA, PDLA, blend of PLLA/PDLA and Sc-PLA solutions (inset: spectra in the wavenumber range of 960–880 cm^{-1})

that melting enthalpy of the nascent electrospun PLA yarn in Fig. 3, as determined by DSC, was related to recrystallization during DSC testing.

To realize stereocomplex formation in the electrospun PLA yarns, annealing was carried out at 80 °C for 2 h, as suggested in previous research [31]. Figure 4b gives the obtained results for the heat-treated samples. As can be seen, two distinguished bands appeared. Only one band was appeared in the spectra of the PLLA, PLDA, and PLLA/PDLA samples at 921 cm^{-1} which was assigned to the α-helix of an enantiomeric PLA. In contrast, for Sc-PLA, a band at 908 cm^{-1} was detected, which was related to the β-helix of the stereocomplex crystals [32–35].

According to FTIR results, it can be said that stereocomplex crystals were not produced during electrospinning of the PLLA/PDLA solutions due to limitation of the molecular mobility as was described in literatures [17, 31]. Upon heat treatment, enough molecular mobility was provided, and thereby, the PLLA, PDLA, and PLLA/PDLA electrospun fibers were only crystallized into homocrystals, whereas stereocomplex crystals were only formed in the Sc-PLA electrospun yarns. The formation of stereocomplex crystals is mainly attributed to the interactions between the methyl and carbonyl groups intermolecular ordering between PLLA and PDLA chains in the electrospun obtained from PLLA/PDLA solution [31]. In other words, before heat treatment, there was only precursor but no stereocomplex crystals. Thus, no peak was observed at 908 cm^{-1}. But after heat treatment, the precursors were transformed into stereocomplex crystals via molecular reorganization, and thereby, the characteristic band appeared at 908 cm^{-1}.

Wide-angle X-ray diffraction

Wide-angle X-ray diffraction (WAXD) analysis was performed to investigate the crystalline structure of the electrospun yarn samples. Figure 5 shows the XRD profiles of the heat-treated PLLA, PDLA, PLLA/PDLA, and Sc-PLA electrospun yarns. For the heat-treated PLLA, PDLA, and PLLA/PDLA electrospun yarns, two crystalline reflections

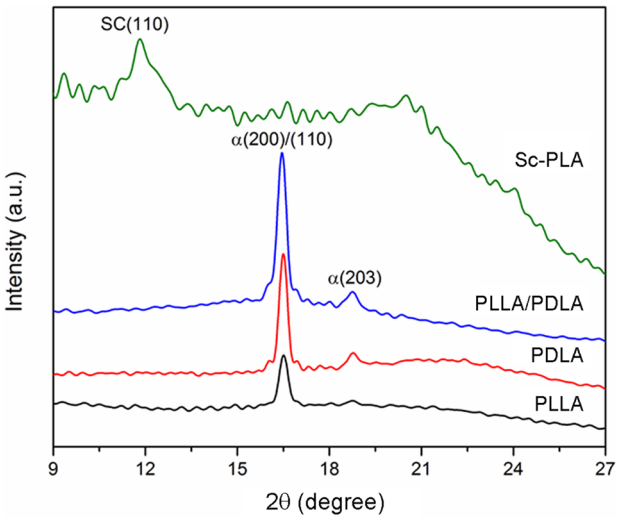

Fig. 5 WAXD profiles of the electrospun yarns obtained from PLLA, PDLA, blend of PLLA/PDLA and Sc-PLA solutions after heat treatment at 80 °C for 2 h

at 2θ values of 16.9° and 19.1° were observed, assigning to the (200)/(110) and (203) diffraction planes of PLA homocrystals [36, 37]. In contrast, the heat-treated Sc-PLA electrospun yarn showed a diffraction peak at a 2θ value of 12.0°, which is assigned to the (110) plane of PLA stereocomplex crystal [36, 37]. No crystalline peak relating to PLA homocrystals appeared for the Sc-PLA sample, which supporting the FTIR results.

Mechanical properties

The mechanical behavior of the electrospun fibrous structures depends on several factors, such as processing conditions, their composition, fiber structure, individual properties of fiber constituents, and fiber interaction [28, 38, 39]. Compared to the fibrous webs, twisted yarns exhibited enhanced cohesion and friction between fibers and thus showed improved mechanical performance.

The mechanical properties (stress-at-break, Young's modulus, and strain-at-break) of the PLA-based electrospun yarns were considered by stress–strain measurements. The results are presented in Table 3, and typical stress–strain curves are demonstrated in Fig. 6.

This study clearly shows that stereocomplexation process significantly affects the mechanical performance of the electrospun yarns. As can be seen, in the case of electrospun Sc-PLA yarns, higher mechanical properties were observed compared to PLLA, PDLA, or hybrid yarns (Fig. 6). At the same condition, the PLLA electrospun yarns had the stress-at-break and Young's modulus of 2.66 and 24.68 cN/tex, respectively, and strain-at-break of 180%, while, Sc-PLA yarns exhibited relatively higher values of stress-at-break

Table 3 Mechanical properties of PLA electrospun yarns

Yarn Sample	Stress-at-break (cN/tex)	Young's modulus (cN/tex)	Strain-at-break (%)
PLLA	2.66 ± 0.29	24.68 ± 3.83	180.40 ± 34.03
PDLA	2.54 ± 0.28	27.94 ± 1.52	166.78 ± 21.02
Hybrid PLLA/PDLA	2.54 ± 0.19	31.93 ± 3.07	143.77 ± 22.40
Sc-PLA	3.35 ± 0.14	50.08 ± 2.86	125.40 ± 16.37

(3.35 cN/tex), and Young's modulus (50.08 cN/tex) than those of the PLLA and PDLA yarns (Table 3). But, Sc-PLA electrospun yarns showed lower strain-at-break of 125%. The formation of stereocomplex crystalline structure resulted from the strong interaction between the l-lactide acid and the d-lactide acid within the fibers likely led to the higher stress-at-break and Young's modulus for electrospun Sc-PLA yarns [18, 40]. These findings are in good agreement with the other research reports [16, 41, 42].

It is reported that diameter of the fibers may influence the mechanical properties. Also, the mechanical performance of the fibrous materials, in addition to the characteristics of the individual fibers, depending on the geometry resulted from fiber orientation within the structure, and interaction and cohesive forces between fibers [29, 43, 44]. Therefore, the increased values of stress-at-break and modulus for fibers with decreased diameters can also be due to the higher orientation of the molecular chains in thinner fibers. Moreover, fibers with a smaller diameter have a higher surface area to volume ratio. More contact area between fibers in the yarn structure can result in increased mechanical properties [28, 29].

Figure 7 shows the fracture morphology of a Sc-PLA yarn after being pulled to failure under tension. The plastic

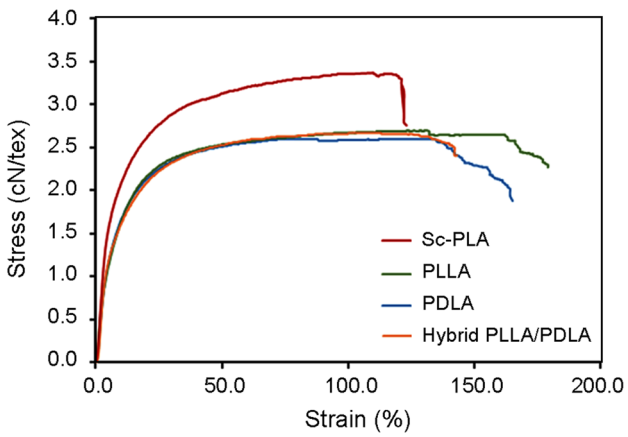

Fig. 6 Stress–strain curves of PLA-based electrospun yarns

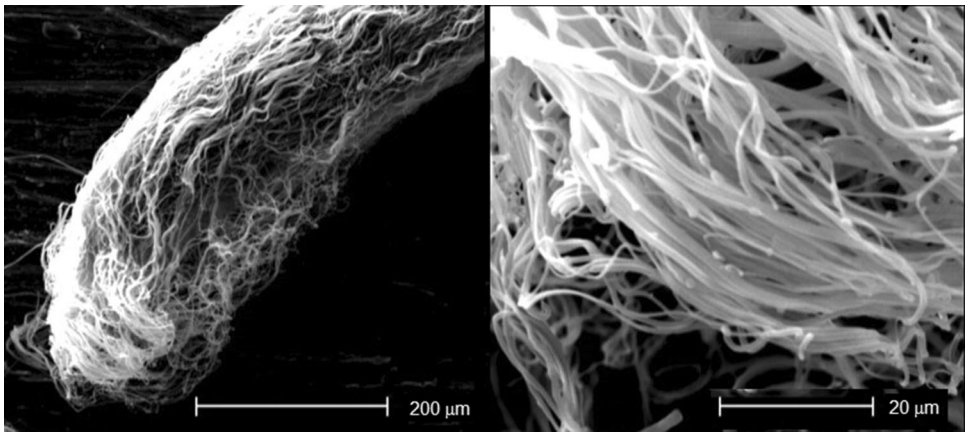

Fig. 7 SEM micrographs prepared from the end failure of the electrospun Sc-PLA yarn under tensile loading

deformation, buckling, and necks are clearly visible in these micrographs.

Conclusion

In this work, it was shown that the electrospinning of the stereocomplexed twisted yarns is able to improve the physical and mechanical performance of the PLA-based nanofibrous structures for their potential applications as medical devices. An electrospinning setup equipped with two nozzles was applied to produce stereocomplex PLA twisted yarns in a continuous process from a blend solution of high molecular weight PLLA and PDLA at an equal ratio of 1:1. The characterization observations showed that uniform yarns composed of bead-free fibers were obtained, and compared to PLLA or PDLA samples, their stereocomplexed fibers and yarns had significantly smaller diameters. DSC analysis of the yarns revealed that the presence of stereocomplex crystallites in the Sc-PLA significantly improved the melting temperature by about 56 ° C than the PLA's homocrystallites. Moreover, the formation of stereocomplex crystals and homocrystals upon heat treatment were confirmed via FTIR analysis by the appearance of the characteristic absorption band at 908 cm^{-1} and 921 cm^{-1}, respectively. The WAXD patterns of the heat-treated electrospun yarns also supported the FTIR results. The stereocomplex formation also affected the mechanical performance of the electrospun yarns. Compared to the PLLA or PDLA samples, the stress-at-break and Young's modulus of electrospun stereocomplex PLA yarns increased, while the strain-at-break decreased.

Acknowledgements H Maleki sincerely thanks the Ministry of Science, Research and Technology of the Islamic Republic of Iran and University of Sistan and Baluchestan, Iran for providing financial support for this work (contract number 982/201/25483). H Maleki also acknowledges the University of Birjand, Iran for providing the research facilities. A Nazir thanks the Pakistan Science Foundation for providing funding and coordination support for this project.

References

1. Lopresti F, Carfì Pavia F, Vitrano I, Kersaudy-Kerhoas M, Brucato V, La Carrubba V (2020) Effect of hydroxyapatite concentration and size on morpho-mechanical properties of PLA-based randomly oriented and aligned electrospun nanofibrous mats. J Mech Behav Biomed Mater 101:103449. https://doi.org/10.1016/j.jmbbm.2019.103449
2. Han J, Xiong L, Jiang X, Yuan X, Zhao Y, Yang D (2019) Biofunctional electrospun nanomaterials: From topology design to biological applications. Prog Polym Sci 91:1–28. https://doi.org/10.1016/j.progpolymsci.2019.02.006
3. Alam F, Shukla VR, Varadarajan KM, Kumar S (2020) Micro-architected 3D printed polylactic acid (PLA) nanocomposite scaffolds for biomedical applications. J Mech Behav Biomed Mater 103:103576. https://doi.org/10.1016/j.jmbbm.2019.103576
4. Brzeziński M, Kost B, Wedepohl S, Socka M, Biela T, Calderón M (2019) Stereocomplexed PLA microspheres: Control over morphology, drug encapsulation and anticancer activity. Colloid Surface B 184:110544. https://doi.org/10.1016/j.colsurfb.2019.110544
5. Wang C, Feng N, Chang F, Wang J, Yuan B, Cheng Y, Liu H, Yu J, Zou J, Ding J, Chen X (2019) Injectable cholesterol-enhanced stereocomplex polylactide thermogel loading chondrocytes for optimized cartilage regeneration. Adv Healthc Mater 8:1900312. https://doi.org/10.1002/adhm.201900312
6. Verma M, Biswal AK, Dhingra S, Gupta A, Saha S (2019) Antibacterial response of polylactide surfaces modified with hydrophilic polymer brushes. Iran Polym J 28:493–504. https://doi.org/10.1007/s13726-019-00717-3
7. Ikada Y, Jamshidi K, Tsuji H, Hyon SH (1987) Stereocomplex formation between enantiomeric poly(lactides). Macromolecules 20:904–906. https://doi.org/10.1021/ma00170a034
8. Bertin A (2012) Emergence of polymer stereocomplexes for biomedical applications. Macromol Chem Phys 213:2329–2352. https://doi.org/10.1002/macp.201200143
9. Brzeziński M, Biela T (2015) Micro- and nanostructures of polylactide stereocomplexes and their biomedical applications. Polym Int 64:1667–1675. https://doi.org/10.1002/pi.4961
10. Shi X, Jing Z, Zhang G (2018) Influence of PLA stereocomplex crystals and thermal treatment temperature on the rheology and crystallization behavior of asymmetric poly(L-Lactide)/poly(D-lactide) blends. J Polym Res 25:71. https://doi.org/10.1007/s10965-018-1467-9
11. Xu J-Z, Li Y, Li Y-K, Chen Y-W, Wang R, Liu G, Liu S-M, Ni H-W, Li Z-M (2018) Shear-induced stereocomplex cylindrites in polylactic acid racemic blends: morphology control and

interfacial performance. Polymer (Guildf) 140:179–187. https://doi.org/10.1016/j.polymer.2018.02.048
12. Xie Y, Lan X-R, Bao R-Y, Lei Y, Cao Z-Q, Yang M-B, Yang W, Wang Y-B (2018) High-performance porous polylactide stereocomplex crystallite scaffolds prepared by solution blending and salt leaching. Mater Sci Eng C 90:602–609. https://doi.org/10.1016/j.msec.2018.05.023
13. Gao X-R, Niu B, Hua W-Q, Li Y, Xu L, Wang Y, Ji X, Zhong G-J, Li Z-M (2018) Rapid preparation and continuous processing of polylactide stereocomplex crystallite below its melting point. Polym Bull 76:3371–3385. https://doi.org/10.1007/s00289-018-2544-2
14. Pan G, Xu H, Mu B, Ma B, Yang Y (2018) A clean approach for potential continuous mass production of high-molecular-weight polylactide fibers with fully stereo-complexed crystallites. J Clean Prod 176:151–158. https://doi.org/10.1016/j.jclepro.2017.12.096
15. Chuan D, Fan R, Wang Y, Ren Y, Wang C, Du Y, Zhou L, Yu J, Gu Y, Chen H, Guo G (2020) Stereocomplex poly(lactic acid)-based composite nanofiber membranes with highly dispersed hydroxyapatite for potential bone tissue engineering. Compos Sci Technol 192:108107. https://doi.org/10.1016/j.compscitech.2020.108107
16. Tsuji H (2016) Poly(lactic acid) stereocomplexes: a decade of progress. Adv Drug Deliv Rev 107:97–135. https://doi.org/10.1016/j.addr.2016.04.017
17. Tsuji H, Nakano M, Hashimoto M, Takashima K, Katsura S, Mizuno A (2006) Electrospinning of Poly(lactic acid) Stereocomplex Nanofibers. Biomacromol 7:3316–3320. https://doi.org/10.1021/bm060786e
18. Kurokawa N, Hotta A (2018) Thermomechanical properties of highly transparent self-reinforced polylactide composites with electrospun stereocomplex polylactide nanofibers. Polymer (Guildf) 153:214–222. https://doi.org/10.1016/j.polymer.2018.08.018
19. Mei L, Ren Y, Gu Y, Li X, Wang C, Du Y, Fan R, Gao X, Chen H, Tong A, Zhou L, Guo G (2018) Strengthened and thermally resistant poly(lactic acid)-based composite nanofibers prepared via easy stereocomplexation with antibacterial effects. ACS Appl Mater Interfaces 10:42992–43002. https://doi.org/10.1021/acsami.8b14841
20. Ren Y, Mei L, Gu Y, Zhao N, Wang Y, Fan R, Tong A, Chen H, Yang H, Han B, Guo G (2019) Stereocomplex crystallite-based eco-friendly nanofiber membranes for removal of Cr(VI) and antibacterial effects. ACS Sustain Chem Eng 7:16072–16083. https://doi.org/10.1021/acssuschemeng.9b02828
21. Kost B, Svyntkivska M, Brzeziński M, Makowski T, Piorkowska E, Rajkowska K, Kunicka-Styczyńska A, Biela T (2020) PLA/β-CD-based fibres loaded with quercetin as potential antibacterial dressing materials. Colloid Surface B 190:110949. https://doi.org/10.1016/j.colsurfb.2020.110949
22. Paneva D, Spasova M, Stoyanova N, Manolova N, Rashkov I (2019) Electrospun fibers from polylactide-based stereocomplex: why? Int J Polym Mater Polym Biomater. https://doi.org/10.1080/00914037.2019.1706516
23. Ishii D, Ying TH, Mahara A, Yamaoka T, Lee W, Iwata T, Murakami S (2009) In vivo tissue response and degradation behavior of PLLA and stereocomplexed PLA nanofibers. Biomacromol 10:237–242. https://doi.org/10.1021/bm8009363
24. Wu S, Zhou R, Zhou F, Streubel PN, Chen S, Duan B (2020) Electrospun thymosin Beta-4 loaded PLGA/PLA nanofiber/microfiber hybrid yarns for tendon tissue engineering application. Mater Sci Eng C 106:110268. https://doi.org/10.1016/j.msec.2019.110268
25. Asghari Mooneghi S, Gharehaghaji AA, Hosseini-Toudeshky H, Torkaman G (2019) Effect of fatigue loading on wicking properties of polyamide 66 nanofiber yarns. J Appl Polym Sci 136:47206. https://doi.org/10.1002/app.47206
26. Maleki H, Gharehaghaji AA, Toliyat T, Dijkstra PJ (2016) Drug release behavior of electrospun twisted yarns as implantable medical devices. Biofabrication 8:35019. https://doi.org/10.1088/1758-5090/8/3/035019
27. Semnani Rahbar R, Maleki H, Kalantari B (2016) Fabrication of electrospun nanofibre yarn based on nylon 6/microencapsulated phase change materials. J Exp Nanosci 11:1402–1415. https://doi.org/10.1080/17458080.2016.1233582
28. Maleki H, Gharehaghaji AA, Dijkstra PJ (2017) Electrospinning of continuous poly (L-lactide) yarns: effect of twist on the morphology, thermal properties and mechanical behavior. J Mech Behav Biomed Mater 71:231–237. https://doi.org/10.1016/j.jmbbm.2017.03.031
29. Maleki H, Gharehaghaji AA, Moroni L, Dijkstra PJ (2013) Influence of the solvent type on the morphology and mechanical properties of electrospun PLLA yarns. Biofabrication 5:035014. https://doi.org/10.1088/1758-5082/5/3/035014
30. Maleki H, Mathur S, Klein A (2020) Antibacterial Ag containing core-shell polyvinyl alcohol-poly (lactic acid) nanofibers for biomedical applications. Polym Eng Sci 60:1221–1230. https://doi.org/10.1002/pen.25375
31. Zhang P, Tian R, Na B, Lv R, Liu Q (2015) Intermolecular ordering as the precursor for stereocomplex formation in the electrospun polylactide fibers. Polymer 60:221–227. https://doi.org/10.1016/j.polymer.2015.01.049
32. Zhang J, Sato H, Tsuji H, Noda I, Ozaki Y (2005) Infrared spectroscopic study of CH_3···OC interaction during poly(L-lactide)/poly(D-lactide) stereocomplex formation. Macromolecules 38:1822–1828. https://doi.org/10.1021/ma047872w
33. Biedroń T, Brzeziński M, Biela T, Kubisa P (2012) Microspheres from stereocomplexes of polylactides containing ionic liquid end-groups. J Polym Sci A Polym Chem 50:4538–4547. https://doi.org/10.1002/pola.26266
34. Brzeziński M, Seiffert S (2015) Monodisperse microspheres from supramolecular complexing polylactides. Mater Lett 161:471–475. https://doi.org/10.1016/j.matlet.2015.09.008
35. Brzezinski M, Bogusławska M, Ilcikova M, Mosnacek J, Biela T (2012) Unusual thermal properties of polylactides and polylactide stereocomplexes containing polylactide-functionalized multi-walled carbon nanotubes. Macromolecules 45:8714–8721. https://doi.org/10.1021/ma301554q
36. Bai L, Zhang Z-M, Pu J-H, Feng C-P, Zhao X, Bao R-Y, Liu Z-Y, Yang M-B, Yang W (2020) Highly thermally conductive electrospun stereocomplex polylactide fibrous film dip-coated with silver nanowires. Polymer (Guildf) 194:122390. https://doi.org/10.1016/j.polymer.2020.122390
37. Bao RY, Yang W, Jiang W-R, Liu Z-Y, Xie B-H, Yang M-B (2013) Polymorphism of racemic poly(L-lactide)/poly (D-lactide) blend: effect of melt and cold crystallization. J Phys Chem B 117:3667–3674. https://doi.org/10.1021/jp311878f
38. Picciani PHS, Medeiros ES, Pan Z, Wood DF, Orts WJ, Mattoso LHC, Soares BG (2010) Structural, electrical, mechanical, and thermal properties of electrospun poly(lactic acid)/polyaniline blend fibers. Macromol Mater Eng 295:618–627. https://doi.org/10.1002/mame.201000019
39. Maleki H, Barani H (2018) Morphological and mechanical properties of drawn poly(L-lactide) electrospun twisted yarns. Polym Eng Sci 58:1091–1096. https://doi.org/10.1002/pen.24671
40. Jing Y, Quan C, Liu B, Jiang Q, Zhang C (2016) A mini review on the functional biomaterials based on poly(lactic acid) stereocomplex. Polym Rev 56:262–286. https://doi.org/10.1080/15583724.2015.1111380
41. Zhang X, Nakagawa R, Chan KHK, Kotaki M (2012) Mechanical property enhancement of polylactide nanofibers through optimization of molecular weight, electrospinning conditions,

and stereocomplexation. Macromolecules 45:5494–5500. https://doi.org/10.1021/ma300289z
42. Jing Y, Zhang L, Huang R, Bai D, Bai H, Zhang Q, Fu Q (2017) Ultrahigh-performance electrospun polylactide membranes with excellent oil/water separation ability: via interfacial stereocomplex crystallization. J Mater Chem A 5:19729–19737. https://doi.org/10.1039/c7ta05379g
43. Baker SR, Banerjee S, Bonin K, Guthold M (2016) Determining the mechanical properties of electrospun poly-ε-caprolactone (PCL) nanofibers using AFM and a novel fiber anchoring technique. Mater Sci Eng C 59:203–212. https://doi.org/10.1016/j.msec.2015.09.102
44. Domingues RMA, Chiera S, Gershovich P, Motta A, Reis RL, Gomes ME (2016) Enhancing the biomechanical performance of anisotropic nanofibrous scaffolds in tendon tissue engineering: reinforcement with cellulose nanocrystals. Adv Healthc Mater 5:1364–1375. https://doi.org/10.1002/adhm.201501048